Synthesis and Reactions of the Triruthenamonocarboncarborane Cluster Complex $[NHMe_3][Ru_3(CO)_8(\eta^5\text{-}7\text{-}CB_{10}H_{11})]$†

Dianne D. Ellis, Andreas Franken, and F. Gordon A. Stone*

Department of Chemistry, Baylor University, Waco, Texas 76798-7348

Received February 24, 1999

In thf (tetrahydrofuran) at reflux temperatures the compounds $[Ru_3(CO)_{12}]$ and $[NHMe_3]$-[*nido*-7-$CB_{10}H_{13}$] give the anionic triruthenium complex $[Ru_3(CO)_8(\eta^5\text{-}7\text{-}CB_{10}H_{11})]^-$, characterized as its $[PPh_4]^+$ salt (**4a**). Protonation of $[NHMe_3][Ru_3(CO)_8(\eta^5\text{-}7\text{-}CB_{10}H_{11})]$ (**4b**) with HBF_4·Et_2O yields the hydrido cluster complex $[Ru_3(\mu\text{-}H)(CO)_8(\eta^5\text{-}7\text{-}CB_{10}H_{11})]$ (**5**), the structure of which has been determined by X-ray diffraction. The molecule has a triangle of ruthenium atoms. One ruthenium atom is ligated by the η^5-7-$CB_{10}H_{11}$ cage system and carries two CO groups, while the other two ruthenium atoms each carry three CO molecules with a hydrido ligand bridging the metal−metal bond which joins them. In addition, these two metal atoms are linked to the cage through two exopolyhedral B−H⇀Ru bonds. These are formed using boron atoms lying in β sites with respect to the carbon in the open CB*BB*B face of the *nido*-$CB_{10}H_{11}$ fragment ligating the $Ru(CO)_2$ group. Treatment of **4b** in thf with $[CuCl(PPh_3)_3]$ in the presence of $TlPF_6$, or with $Ag[BF_4]$ and PPh_3, affords the bimetallic complexes $[Ru_3(\mu\text{-}H)(CO)_7(PPh_3)\{\eta^5\text{-}10\text{-}M(PPh_3)\text{-}7\text{-}CB_{10}H_{10}\}]$ (M = Cu (**6a**), Ag (**6b**)), respectively. The structure of **6a** was established by X-ray diffraction. A triangle of ruthenium atoms is formed by $Ru(CO)_2$, $Ru(CO)_3$, and $Ru(CO)_2(PPh_3)$ units. This triangle is bridged by a *nido*-10-$Cu(PPh_3)$-7-$CB_{10}H_{10}$ fragment, the open CBBBB face of which is η^5-coordinated to the $Ru(CO)_2$ group. The two boron atoms lying in the β-sites in the CB*BB*B ring coordinated to the $Ru(CO)_2$ moiety form exopolyhedral B−H ⇀ Ru and B−Cu→Ru linkages, respectively, to the $Ru(CO)_2(PPh_3)$ and $Ru(CO)_3$ groups, which have their Ru−Ru bond bridged by a hydrido ligand. A novel feature of the structure is a three-center−two-electron B−H⇀Cu bond involving the B(2) site in the *nido*-10-$Cu(PPh_3)$-7-$CB_{10}H_{10}$ cage system. The reaction between **4b** and $[AuCl(PPh_3)]$ gives $[Ru_3(\mu\text{-}H)(CO)_8\{\eta^5\text{-}10\text{-}Au(PPh_3)\text{-}7\text{-}CB_{10}H_{10}\}]$ (**6c**), the structure of which was also determined by X-ray crystallography. It is similar to that of **6a**, except there is no exopolyhedral B−H⇀Au bond supplementing the B(10)−Au→Ru and Au−P bonds.

Introduction

The carboranes *nido*-7,8-R_2-7,8-$C_2B_9H_{11}$ (R = H, Me) react with $[Ru_3(CO)_{12}]$ in suitable solvents (heptane and CH_2Cl_2) to give in good yield the mono- and triruthenacarboranes $[Ru(CO)_3(\eta^5\text{-}7,8\text{-}R_2\text{-}7,8\text{-}C_2B_9H_9)]$ (R = H (**1a**), Me (**1b**)) and $[Ru_3(CO)_8(\eta^5\text{-}7,8\text{-}Me_2\text{-}7,8\text{-}C_2B_9H_9)]$ (**2**), respectively (Chart 1). These compounds have an extensive derivative chemistry, reacting with substrate molecules at both their ruthenium centers and their BH groups.[1] Dicarbollide ligands have assumed an increasingly important role in organometallic chemistry in recent years, especially as a result of their ability to stabilize an extraordinary variety of polynuclear metal species.[2,3] In contrast, similar studies on the chemistry of complexes with monocarbollide ligands are less developed. In attempting to redress the balance, using a methodology similar to that which led to the species **1** and **2**, we prepared the charge-compensated triruthena- and triosmamonocarboncarborane clusters $[M_3(CO)_8(\eta^5\text{-}7\text{-}NMe_3\text{-}7\text{-}CB_{10}H_{10})]$ (M = Ru (**3a**), Os (**3b**)) by heating *nido*-7-NMe_3-7-$CB_{10}H_{12}$ with the carbonyls $[M_3(CO)_{12}]$ in toluene.[4] Herein we report further studies on monocarbollide metal complexes based on reacting

† The compounds described in this paper have ruthenium atoms incorporated into either *closo*-1,2-dicarba-3-ruthenadodecaborane or *closo*-1-carba-2-ruthenadodecaborane frameworks. However, to avoid a complicated nomenclature for the complexes reported, and to relate them to the many known ruthenium species with η^5-coordinated cyclopentadienyl ligands, we treat the cages as *nido* 11-vertex ligands with numbering as for an icosahedron from which the 12th vertex has been removed.

(1) (a) Anderson, S.; Mullica, D. F.; Sappenfield, E. L.; Stone, F. G. A. *Organometallics* **1995**, *14*, 3516. (b) Anderson, S.; Mullica, D. F.; Sappenfield, E. L.; Stone, F. G. A. *Organometallics* **1996**, *15*, 1676. (c) Liao, Y.-H.; Mullica, D. F.; Sappenfield, E. L.; Stone, F. G. A. *Organometallics* **1996**, *15*, 5102. (d) Anderson, S.; Jeffery, J. C.; Liao, Y.-H.; Mullica, D. F.; Sappenfield, E. L.; Stone, F. G. A. *Organometallics* **1997**, *16*, 958. (e) Jeffery, J. C.; Jelliss, P. A.; Liao, Y.-H.; Stone, F. G. A. *J. Organomet. Chem.* **1998**, *551*, 27. (f) Jeffery, J. C.; Jelliss, P. A.; Psillakis, E.; Rudd, G. E. A.; Stone, F. G. A. *J. Organomet. Chem.* **1998**, *562*, 17. (g) Ellis, D. D.; Farmer, J. M.; Malget, J. M.; Mullica, D. F.; Stone, F. G. A. *Organometallics* **1998**, *17*, 5540. (h) Jeffery, J. C.; Jelliss, P. A.; Rudd, G. E. A.; Sakanishi, S.; Stone, F. G. A.; Whitehead, J. *J. Organomet. Chem.* **1999**, in press.

(2) Grimes, R. N. In *Comprehensive Organometallic Chemistry II*; Abel, E. W., Stone, F. G. A., Wilkinson, G., Eds.; Pergamon Press: Oxford, U.K., 1995; Vol. 1 (Housecroft, C. E., Ed.), Chapter 9.

(3) Jelliss, P. A.; Stone, F. G. A. *J. Organomet. Chem.* **1995**, *500*, 307.

10.1021/om990133x CCC: $18.00
Publication on Web 06/07/1999

Chart 1

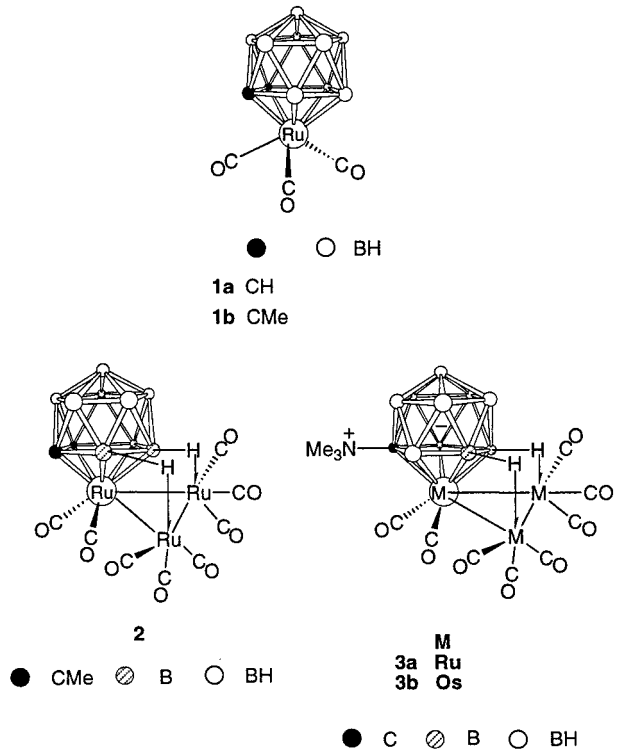

Chart 2

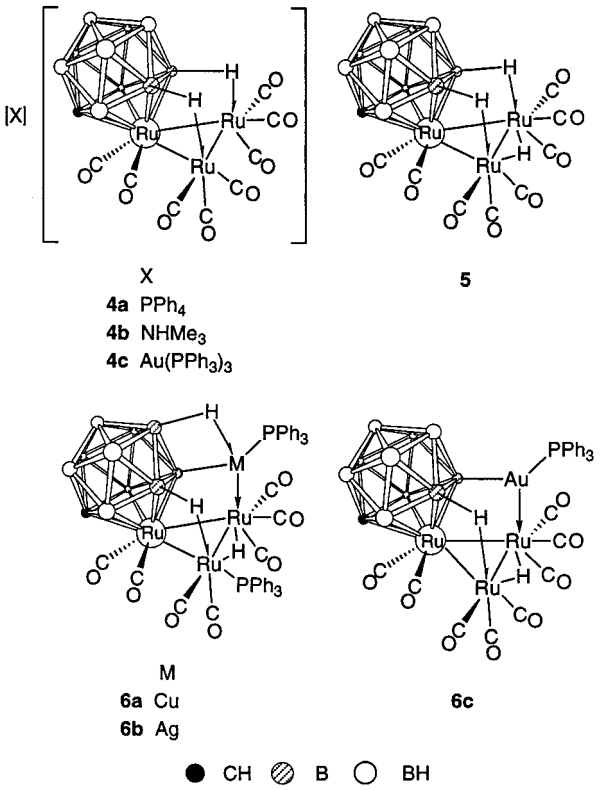

$[NHMe_3][nido\text{-}7\text{-}CB_{10}H_{13}]$ with $[Ru_3(CO)_{12}]$. The anion $[nido\text{-}7\text{-}CB_{10}H_{13}]^-$ is isolobal with the carboranes *nido*-7,8-R_2-7,8-$C_2B_9H_{11}$ (R = H, Me); hence, it seemed likely that salts of this anion would react in a similar manner with $[Ru_3(CO)_{12}]$ to yield ruthenacarborane species. Moreover, the complexes formed would be anionic in nature, thus opening up the possibility of new chemistry through their reactions with electrophiles.

Results and Discussion

The salt $[PPh_4][Ru_3(CO)_8(\eta^5\text{-}7\text{-}CB_{10}H_{11})]$ (**4a**; Chart 2) is formed when $[Ru_3(CO)_{12})]$ and $[NHMe_3][nido\text{-}7\text{-}CB_{10}H_{13}]$ are heated in thf (tetrahydrofuran) to reflux temperatures, followed by addition of $[PPh_4]Br$. The $[NHMe_3]^+$ salt **4b** is an intermediate in the synthesis, but it is difficult to obtain pure, though it can be conveniently used in further preparative work as described below. Data characterizing **4a** are given in Tables 1−3. The ^1H NMR spectrum was informative, displaying a diagnostic quartet resonance (J(BH) = 68 Hz) for the B−H⇀Ru groups at δ −10.63.[5] Correspondingly, there was a signal for these groups at δ 18.8 in the $^{11}B\{^1H\}$ NMR spectrum, which became a doublet (J(HB) = 67 Hz) in a fully coupled ^{11}B spectrum. The $^{13}C\{^1H\}$ NMR spectrum of **4a** revealed a resonance for the cage CH group at δ 33.9.[5] These data, along with a 2:1:1:2:2:2 pattern in the $^{11}B\{^1H\}$ NMR spectrum, indicate that a mirror plane is present. The latter encompasses the cage Ru and C atoms and the midpoint of the $(OC)_3Ru-Ru(CO)_3$ bond. This allows an unambiguous assignment of **4a** as the β,β-isomer; i.e., both B−H⇀Ru bonds involve boron atoms which lie in positions β to the cage carbon vertexes in the CB*BB*B ring ligating the Ru atom.

Protonation of **4b** with $HBF_4 \cdot Et_2O$ affords the neutral complex $[Ru_3(\mu\text{-}H)(CO)_8(\eta^5\text{-}7\text{-}CB_{10}H_{11})]$ (**5**). A single-crystal X-ray diffraction study was carried out to establish the structure. The molecule is shown in Figure 1 , and selected internuclear distances and angles are listed in Table 4. The metal atoms form an isosceles triangle (Ru(1)−Ru(2) = 2.7545(8) Å, Ru(1)−Ru(3) = 2.7596(7) Å, Ru(2)−Ru(3) = 2.9877(7) Å). There is a hydrido ligand H(23) bridging the Ru(2)−Ru(3) bond, which was located in difference Fourier syntheses, and in accord with the presence of this edge-bridging group Ru(2)−Ru(3) is the longer metal−metal bond in the triangle.[6] While the cage system is η^5-coordinated to Ru(1), it bridges the metal triangle with B−H⇀Ru bonds from B(3) to Ru(2) (2.367(5) Å) and from B(4) to Ru(3) (2.360(5) Å). The positions of H(3) and H(4) were located and refined. Atom Ru(1) carries two terminal CO molecules, and Ru(2) and Ru(3) have three each. The bonding of the carborane cage system to the Ru_3 group in **5** is similar to the attachment of the cage fragments to the ruthenium clusters in **2** and **3**.

The NMR data for **5** (Tables 2 and 3) are in complete agreement with the structure established by the X-ray diffraction study. In the ^1H NMR spectrum a diagnostic resonance for the μ-H(23) ligand is seen at δ −19.03.[7] A quartet with broad peaks at δ −10.31 (J(BH) = 56 Hz), corresponding in intensity to two protons, may be assigned to the two B−H⇀Ru linkages, and a further signal at δ 2.32 of relative intensity corresponding to

(4) Lebedev, V. N.; Mullica, D. F.; Sappenfield, E. L.; Stone, F. G. A. *Organometallics* **1996**, *15*, 1669. Lebedev, V. N.; Mullica, D. F.; Sappenfield, E. L.; Stone, F. G. A. *J. Organomet. Chem.* **1997**, *536*−*537*, 537.

(5) Brew, S. A.; Stone, F. G. A. *Adv. Organomet. Chem.* **1993**, *35*, 135.

(6) Teller, R. G.; Bau, R. *Struct. Bonding* **1981**, *44*, 1.

(7) Kaesz, H. D.; Saillant, R. B. *Chem. Rev.* **1972**, *72*, 231.

Table 1. Analytical and Physical Data

compd	color	yield/%	ν_{max}(CO)[a]/cm^{-1}	anal./%[b] C	H
[PPh$_4$][Ru$_3$(CO)$_8$(η^5-7-CB$_{10}$H$_{11}$)] (**4a**)	red	90	2070 s, 2041 s, 2009 s, 1999 s, 1976 s	40.8 (39.4)	3.2 (3.0)
[Ru$_3$(μ-H)(CO)$_8$(η^5-7-CB$_{10}$H$_{11}$)] (**5**)	orange	81	2130 s, 2106 s, 2065 s	16.6 (16.1)[c]	1.9 (1.9)
[Ru$_3$(μ-H)(CO)$_7$(PPh$_3$){η^5-10-Cu(PPh$_3$)-7-CB$_{10}$H$_{10}$}] (**6a**)	orange	41	2070 s, 2061 s, 2047 s, 1993 s	41.3 (41.4)[c]	3.2 (3.3)
[Ru$_3$(μ-H)(CO)$_7$(PPh$_3$){η^5-10-Ag(PPh$_3$)-7-CB$_{10}$H$_{10}$}] (**6b**)	red	38	2106 s, 2070 s, 2041 s, 2005 s	40.1 (40.7)[c]	3.4 (3.2)
[Ru$_3$(μ-H)(CO)$_8${η^5-10-Au(PPh$_3$)-7-CB$_{10}$H$_{10}$}] (**6c**)	dark red	62	2112 s, 2076 s, 2041 s, 2011 s	29.2 (29.0)	2.4 (2.4)

[a] Measured in CH_2Cl_2; medium-intensity bands observed at ca. 2550 cm^{-1} in the spectra of all compounds are due to B−H adsorptions. [b] Calculated values are given in parentheses. [c] Crystallizes with one molecule of CH_2Cl_2.

Table 2. ^{1}H and ^{13}C NMR Data[a]

compd	^{1}H/δ[b]	^{13}C/δ[c]
4a	−10.63 (br q, 2 H, B−H→Ru, J(BH) = 68), 2.10 (s, 1 H, cage CH), 7.60−7.94 (m, 20 H, Ph)	204.4, 201.4, 193.4, 190.5 (CO), 130.8−136.0 (Ph), 33.9 (cage CH)
5	−19.03 (s, 1 H, μ-H), −10.31 (br q, 2 H, B−H→Ru, J(BH) = 56), 2.32 (s, 1 H, cage CH)	198.6, 192.9, 184.5, 179.9 (CO), 39.1 (cage CH)
6a[d]	−18.31 (d, 1 H, μ-H, J(PH) = 13), −9.61 (br q, 1 H, B−H→Ru, J(BH) = 50), 2.31 (s, 1 H, cage CH), 7.24−7.48 (m, 30 H, Ph)	201.5−181.0 (CO), 129.1−133.9 (Ph), 38.1 (cage CH)[e]
6b[d]	−19.61 (d, 1 H, μ-H, J(PH) = 11), −10.24 (br q, 1 H, B−H→Ru, J(BH) = 47), 2.27 (s, 1 H, cage CH), 7.25−7.54 (m, 30 H, Ph)	198.5 (d, J(PC) = 18), 198.4, 192.9, 189.5 (CO × 2), 184.6 (d, J(PC) = 11), 180.0 (CO), 129.1−134.1 (Ph), 39.2 (cage CH)
6c	−19.03 (s, 1 H, μ-H), −10.32 (br q, 1 H, B−H→Ru, J(BH) = 49), 2.30 (s, 1 H, cage CH), 7.48−7.56 (m, 15 H, Ph)	201.4, 199.6, 196.3 (vbr), 194.8, 192.4 (d, J(PC) = 9), 189.7, 185.8, 181.5 (CO), 129.4−134.4 (Ph), 41.5 (cage CH)

[a] Chemical shifts (δ) in ppm and coupling constants (J) in hertz; measurements at ambient temperatures in CD_2Cl_2. [b] Resonances for terminal BH protons occur as broad unresolved signals in the range δ ca. −1 to 3. [c] ^{1}H-decoupled chemical shifts are positive to high frequency of $SiMe_4$. [d] Signals due to B−H→M (M = Cu, Ag) protons in ^{1}H NMR spectra are not observed due to the dynamic process in solution (see text). [e] Insolubility of the compound prevented resolution of all CO signals.

Table 3. ^{11}B and ^{31}P NMR Data[a]

compd	^{11}B/δ[b]	^{31}P/δ[c]
4a	18.8 (2 B, B−H→Ru, J(HB) = 67), −6.0 (1 B), −9.1 (1 B), −12.4 (2 B), −15.2 (2 B), −20.4 (2 B)	
5	23.4 (2 B, B−H→Ru, J(HB) = 52), 2.5 (1 B), −6.1 (1 B), −7.0 (2 B), −8.6 (2 B), −14.6 (2 B)	
6a	40.8 (1 B, B−Cu), 24.2 (1 B, B−H→Ru, J(HB) = 49), −1.2 (1 B), −7.5 (3 B), −11.9 (1 B), −14.0 (2 B), −17.2 (1 B)	39.9 (RuPPh$_3$), 3.9 (br, CuPPh$_3$)
6b	42.9 (1 B, B−Ag), 25.1 (1 B, B−H→Ru, J(HB) = 46), 0.3 (1 B), −6.9 (2 B), −8.9 (2 B), −10.2 (2 B), −15.3 (1 B)	40.0 (RuPPh$_3$), 13.8 (d × 2, AgPPh$_3$, J(^{109}AgP) = 582, J(^{107}AgP) = 510)
6c	44.8 (1 B, B−Au), 25.0 (1 B, B−H→Ru, J(HB) = 49), 1.5 (1 B), −6.6 (5 B), −13.7 (1 B), −14.9 (1 B)	48.7 (AuPPh$_3$)

[a] Chemical shifts (δ) are in ppm and coupling constants (J) are in Hz; measurements at ambient temperatures in CD_2Cl_2. [b] ^{1}H-decoupled chemical shifts are positive to high frequency of BF_3·Et_2O (external). Signals ascribed to more than one boron nucleus may result from overlapping peaks and do not necessarily indicate symmetry equivalence. The ^{1}H−^{11}B coupling constants (J(HB)) were measured from fully coupled ^{11}B spectra. [c] ^{1}H-decoupled chemical shifts are positive to high frequency of H_3PO_4 (external).

one proton is in the region characteristic for a cage CH.[5] In the ^{11}B{^{1}H} NMR spectrum a resonance at δ 23.4 integrating to 2 B, which became a doublet (J(HB) = 52 Hz) in a fully coupled ^{11}B spectrum, is characteristic of B−H→Ru groups. As with the parent anion **4a**, the presence of a mirror plane of symmetry through the cage Ru(1), C(1), and midpoint of the Ru(2)−Ru(3) bond is reflected in the observed ^{1}H and ^{11}B{^{1}H} NMR data, the latter showing a 2:1:1:2:2:2 set of resonances. This is in agreement with the β,β-configuration established by the X-ray diffraction study.

Since the groups [M(PPh$_3$)]$^+$ (M = Cu, Ag, Au) are isolobal with the proton,[8] it seemed likely that these cations would react with **4b** to afford bimetallic clusters. Accordingly, **4b** was generated in situ in thf and treated with 2 equiv of [CuCl(PPh$_3$)$_3$], with TlPF$_6$ added to remove chloride as insoluble TlCl. This reaction yielded the cluster compound [Ru$_3$(μ-H)(CO)$_7$(PPh$_3$){η^5-10-Cu(PPh$_3$)-7-CB$_{10}$H$_{10}$}] (**6a**), the structure of which was established by an X-ray diffraction study.

(8) Stone, F. G. A. *Angew. Chem., Int. Ed. Engl.* **1984**, *23*, 89.

The molecule has an unusual structure, as shown in Figure 2, and selected structural parameters are listed in Table 5. There is a triangular arrangement of ruthenium atoms (Ru(1)−Ru(2) = 2.7953(10) Å, Ru(1)−Ru(3) = 2.8102(9) Å, Ru(2)−Ru(3) = 3.0065(10) Å), with the longer edge bridged by a hydrido ligand H(23), the position of which was located and refined. The Ru(2)−H(23) and Ru(3)−H(23) distances of 1.76(5) and 1.67(5) Å are typical of such bonds.[6] The metal atom Ru(1) is coordinated by two CO molecules and Ru(3) by three such groups, while Ru(2) carries two CO ligands and a PPh$_3$ molecule. The latter lies transoid to the Ru(1)−Ru(2) bond (Ru(1)−Ru(2)−P(2) = 165.91(5)°). The presence of a Cu(PPh$_3$) substituent on the CB$_{10}$ framework is clearly evident (B(4)−Cu = 2.111(8) Å). The pentagonal open face of the *nido*-10-Cu(PPh$_3$)-7-CB$_{10}$H$_{10}$ moiety ligates Ru(1) in the η^5-manner while also forming exopolyhedral bonds to Ru(2) and Ru(3). The link to Ru(2) is a three-center−two-electron bridge, B(3)−H(3)→Ru(2). Atom H(3) was located and its position refined. The bridge to Ru(3) involves the Cu(PPh$_3$) substituent, which

Table 4. Selected Internuclear Distances (Å) and Angles (deg) for $[Ru_3(\mu\text{-H})(CO)_8(\eta^5\text{-7-}CB_{10}H_{11})]\cdot CH_2Cl_2$ (5)

Ru(1)−C(12)	1.908(5)	Ru(1)−C(11)	1.913(5)	Ru(1)−C(1)	2.258(5)	Ru(1)−B(2)	2.256(5)
Ru(1)−B(4)	2.222(5)	Ru(1)−B(3)	2.242(5)	Ru(1)−B(5)	2.243(5)	Ru(1)−Ru(2)	2.7545(8)
Ru(1)−Ru(3)	2.7596(7)	Ru(2)−H(3)	1.81(6)	Ru(2)−H(23)	1.70(5)	Ru(2)−B(3)	2.367(5)
Ru(2)−C(21)	1.946(5)	Ru(2)−C(22)	1.942(5)	Ru(2)−C(23)	1.905(5)	Ru(2)−Ru(3)	2.9877(7)
Ru(3)−H(4)	1.73(5)	Ru(3)−B(4)	2.360(5)	Ru(3)−C(31)	1.926(5)	Ru(3)−C(32)	1.931(5)
Ru(3)−H(23)	1.77(5)	Ru(3)−C(33)	1.924(5)	C(11)−O(11)	1.143(6)	C(12)−O(12)	1.147(6)
C(21)−O(21)	1.120(6)	C(23)−O(23)	1.131(6)	C(22)−O(22)	1.117(6)	C(31)−O(31)	1.130(6)
C(32)−O(32)	1.123(6)	C(33)−O(33)	1.121(6)				

C(12)−Ru(1)−C(11)	86.6(2)	C(12)−Ru(1)−Ru(2)	81.43(14)	C(11)−Ru(1)−Ru(3)	83.42(14)
C(11)−Ru(1)−Ru(2)	128.5(2)	C(1)−Ru(1)−Ru(2)	129.47(12)	Ru(2)−Ru(1)−Ru(3)	65.62(2)
C(23)−Ru(2)−C(21)	93.0(2)	C(12)−Ru(1)−Ru(3)	126.8(2)	C(22)−Ru(2)−C(21)	94.1(2)
C(22)−Ru(2)−Ru(1)	166.4(2)	C(23)−Ru(2)−C(22)	94.2(2)	C(21)−Ru(2)−Ru(1)	95.38(14)
C(33)−Ru(3)−C(32)	94.7(2)	C(23)−Ru(2)−Ru(1)	95.06(14)	C(22)−Ru(2)−Ru(3)	113.1(2)
C(31)−Ru(3)−Ru(1)	96.8(2)	C(23)−Ru(2)−Ru(3)	88.1(2)	Ru(1)−Ru(2)−Ru(3)	57.27(2)
C(31)−Ru(3)−Ru(2)	153.8(2)	C(21)−Ru(2)−Ru(3)	152.58(14)	C(31)−Ru(3)−C(32)	93.7(2)
O(11)−C(11)−Ru(1)	175.0(5)	C(33)−Ru(3)−C(31)	90.2(2)	C(32)−Ru(3)−Ru(1)	164.04(14)
O(21)−C(21)−Ru(2)	178.3(4)	C(33)−Ru(3)−Ru(1)	97.25(14)	C(32)−Ru(3)−Ru(2)	112.3(2)
O(32)−C(32)−Ru(3)	176.2(4)	C(33)−Ru(3)−Ru(2)	90.7(2)	Ru(1)−Ru(3)−Ru(2)	57.11(2)
O(22)−C(22)−Ru(2)	178.3(5)	O(12)−C(12)−Ru(1)	177.0(5)	O(23)−C(23)−Ru(2)	178.3(4)
O(33)−C(33)−Ru(3)	177.2(4)	O(31)−C(31)−Ru(3)	179.1(4)	Ru(1)−B(3)−Ru(2)	73.3(2)
Ru(1)−B(4)−Ru(3)	74.0(2)				

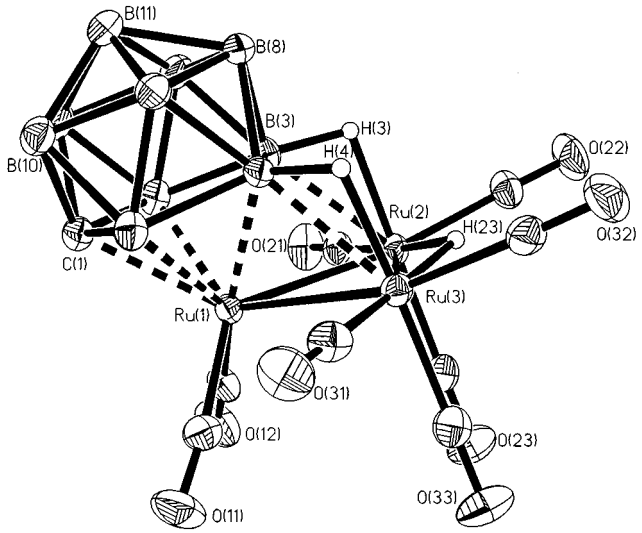

Figure 1. Structure of $[Ru_3(\mu\text{-H})(CO)_8(\eta^5\text{-7-}CB_{10}H_{11})]$ (**5**), showing the crystallographic labeling scheme. Thermal ellipsoids are shown at the 40% probability level. Only the agostic hydrogen atoms H(3) and H(4) and H(23) bridging the Ru(2)−Ru(3) bond are shown for clarity.

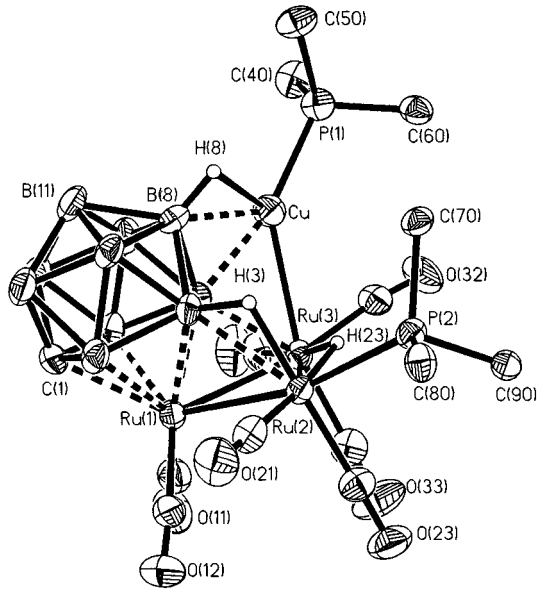

Figure 2. Structure of $[Ru_3(\mu\text{-H})(CO)_7(PPh_3)\{\eta^5\text{-10-Cu-}(PPh_3)\text{-7-}CB_{10}H_{10}\}]$ (**6a**), showing the crystallographic labeling scheme. Thermal ellipsoids are shown at the 40% probability level. Only the agostic hydrogen atoms H(3) and H(8), H(23) bridging the Ru(2)−Ru(3) bond, and the C^1 atoms of the phenyl groups are shown for clarity.

forms a B(4)−Cu→Ru(3) linkage (Ru(3)−Cu = 2.6787(12) Å, Ru(3)−B(4) = 2.221(8) Å). Interestingly, theB(8)−H(8) group partakes in a B(8)−H(8)⇀Cu three-center−two-electron bond with the copper atom (B(8)−Cu = 2.365(8) Å, H(8)−Cu = 2.20(5) Å). Such linkages are well-established for molecules where a B−H⇀Cu interaction supplements a direct bond between the copper and another metal atom M which is a vertex in a *closo*-3,1,2-MC_2B_9 system.[9,10] However, **6a** is unique in having the copper atom σ-bonded to a boron vertex in the η^5-coordinated CBBBB belt of the carborane framework and also forming a B−H⇀Cu linkage with a boron atom in the upper pentagonal B_5 layer of the cage.

The NMR data for **6a** are given in Tables 2 and 3. In solution the molecule evidently undergoes dynamic behavior, since even when measured at −80 °C the ^{1}H NMR spectrum did not reveal a signal for the B−H⇀Cu group. This is not unusual even when such bonds are present.[10a] It is well-established that metal−ligand groups exopolyhedrally attached to icosahedral carborane frameworks by B−H⇀M linkages can undergo exchange mechanisms involving equilibria between tautomers and these processes are fast on the NMR time scale.[11,12] The Cu(PPh_3) moiety in **6a** is held in place by the B(4)−Cu bond; therefore, the likely fluxional

(9) Kang, H. C.; Do, Y.; Knobler, C. B.; Hawthorne, M. F. *Inorg. Chem.* **1988**, *27*, 1716.

(10) (a) Cabioch, J.-L.; Dossett, S. J.; Hart, I. J.; Pilotti, M. U.; Stone, F. G. A. *J. Chem. Soc., Dalton Trans.* **1991**, 519. (b) Batten, S. A.; Jeffery, J. C.; Jones, P. L.; Mullica, D. F.; Rudd, M. D.; Sappenfield, E. L.; Stone, F. G. A.; Wolf, A. *Inorg. Chem.* **1997**, *36*, 2570.

(11) Long, J.; Marder, T. B.; Behnken, P. E.; Hawthorne, M. F. *J. Am. Chem. Soc.* **1984**, *106*, 2979.

(12) (a) Jeffery, J. C.; Ruiz, M. A.; Sherwood, P.; Stone, F. G. A. *J. Chem. Soc., Dalton Trans.* **1989**, 1845. (b) Carr, N.; Gimeno, M. C.; Goldberg, J. E.; Pilotti, M. U.; Stone, F. G. A.; Topaloğlu, I. *J. Chem. Soc., Dalton Trans.* **1990**, 2253. (c) Jeffery, J. C.; Jelliss, P. A.; Stone, F. G. A. *J. Chem. Soc., Dalton Trans.* **1993**, 1073. (d) Jeffery, J. C.; Jelliss, P. A.; Rees, L. H.; Stone, F. G. A. *Organometallics* **1998**, *17*, 2258.

Table 5. Selected Internuclear Distances (Å) and Angles (deg) for $[Ru_3(\mu\text{-H})(CO)_7(PPh_3)\{\eta^5\text{-10-Cu}(PPh_3)\text{-7-}CB_{10}H_{10}\}]\cdot CH_2Cl_2$ (6a)

Ru(1)−C(11)	1.897(9)	Ru(1)−C(12)	1.912(8)	Ru(1)−B(2)	2.255(8)	Ru(1)−B(3)	2.206(8)
Ru(1)−B(4)	2.196(8)	Ru(1)−C(1)	2.294(6)	Ru(1)−B(5)	2.250(8)	Ru(1)−Ru(2)	2.7953(10)
Ru(1)−Ru(3)	2.8102(9)	Ru(2)−H(23)	1.76(5)	Ru(2)−B(3)	2.366(8)	Ru(2)−H(3)	1.70(5)
Ru(2)−C(21)	1.901(8)	Ru(2)−C(23)	1.892(8)	Ru(2)−P(2)	2.337(2)	Ru(2)−Ru(3)	3.0065(10)
Ru(3)−C(31)	1.879(8)	Ru(3)−C(32)	1.882(8)	Ru(3)−C(33)	1.948(9)	Ru(3)−B(4)	2.221(8)
Ru(3)−Cu	2.6787(12)	Ru(3)−H(23)	1.67(5)	C(11)−O(11)	1.148(8)	C(12)−O(12)	1.128(8)
C(21)−O(21)	1.125(8)	C(23)−O(23)	1.127(8)	C(31)−O(31)	1.150(8)	C(32)−O(32)	1.142(8)
C(33)−O(33)	1.125(8)	Cu−P(1)	2.230(2)	B(4)−Cu	2.111(8)	H(8)−Cu	2.20(5)
B(8)−Cu	2.365(8)						

C(11)−Ru(1)−C(12)	84.5(3)	C(11)−Ru(1)−Ru(2)	125.4(2)	C(12)−Ru(1)−Ru(3)	124.5(2)
C(12)−Ru(1)−Ru(2)	80.1(2)	C(11)−Ru(1)−Ru(3)	82.8(2)	Ru(2)−Ru(1)−Ru(3)	64.87(3)
C(23)−Ru(2)−P(2)	90.6(2)	C(23)−Ru(2)−C(21)	91.6(3)	C(21)−Ru(2)−P(2)	93.4(2)
C(21)−Ru(2)−Ru(1)	94.5(2)	C(23)−Ru(2)−Ru(1)	100.8(2)	P(2)−Ru(2)−Ru(1)	165.91(5)
C(21)−Ru(2)−Ru(3)	152.2(2)	Ru(1)−Ru(2)−Ru(3)	57.81(2)	C(23)−Ru(2)−Ru(3)	91.6(2)
C(31)−Ru(3)−C(33)	95.8(3)	C(32)−Ru(3)−C(33)	93.8(3)	P(2)−Ru(2)−Ru(3)	114.20(5)
C(32)−Ru(3)−Cu	69.8(2)	C(33)−Ru(3)−Cu	163.2(2)	C(31)−Ru(3)−C(32)	88.9(3)
C(31)−Ru(3)−Ru(1)	95.2(2)	C(33)−Ru(3)−Ru(1)	96.4(2)	C(31)−Ru(3)−Cu	87.5(3)
C(31)−Ru(3)−Ru(2)	152.6(2)	Cu−Ru(3)−Ru(1)	99.67(3)	B(4)−Ru(3)−Cu	50.0(2)
O(11)−C(11)−Ru(1)	177.2(7)	C(33)−Ru(3)−Ru(2)	87.7(2)	C(32)−Ru(3)−Ru(1)	168.6(2)
O(23)−C(23)−Ru(2)	175.7(7)	Cu−Ru(3)−Ru(2)	96.90(3)	Ru(1)−Ru(3)−Ru(2)	57.32(2)
O(33)−C(33)−Ru(3)	177.7(7)	O(12)−C(12)−Ru(1)	176.3(7)	C(32)−Ru(3)−Ru(2)	118.1(2)
B(4)−Cu−B(8)	46.2(3)	O(31)−C(31)−Ru(3)	177.9(7)	O(21)−C(21)−Ru(2)	178.6(7)
B(8)−Cu−Ru(3)	94.9(2)	Cu−B(4)−Ru(3)	76.3(3)	O(32)−C(32)−Ru(3)	172.7(7)
B(4)−Cu−P(1)	165.7(2)	B(4)−Cu−Ru(3)	53.7(2)	Cu−B(4)−Ru(1)	153.8(4)
P(1)−Cu−Ru(3)	140.54(7)	P(1)−Cu−B(8)	121.8(2)		

process would be a restricted one in which the B−H⇀Cu linkage exchanges between B(8)H(8) and B(9)H(9) vertexes on either side in the same pentagonal layer.[12a,d] In the ^{1}H NMR spectrum the B(3)−H(3)⇀Ru(2) group displays a diagnostic quartet at δ −9.61 (J(BH) = 50 Hz)[5] and a doublet resonance for μ-H(23) is seen at δ −18.31 (J(PH) = 13 Hz).[7] In the ^{11}B{^{1}H} NMR spectrum a signal at δ 40.8, which remains a singlet in the fully coupled ^{11}B NMR spectrum, may be assigned to the B(4)Cu group, while the resonance at δ 24.2 can be attributed to the B(3)H(3) group. It becomes a doublet (J(HB) = 49 Hz) in the ^{11}B NMR spectrum. The ^{31}P-{^{1}H} NMR spectrum shows two resonances, as expected. These are at δ 39.9 and 3.9 and may be assigned on the basis of their chemical shifts to the Ru(PPh_3) and Cu-(PPh_3) groups, respectively. The latter peak is broadened by unresolved ^{11}B−^{31}P coupling.

The reaction between **4b** generated in situ and Ag-[BF_4], to which 1 mol equiv of PPh_3 had been added, afforded the compound $[Ru_3(\mu\text{-H})(CO)_7(PPh_3)\{\eta^5\text{-10-Ag}(PPh_3)\text{-7-}CB_{10}H_{10}\}]$ (**6b**), data for which are given in Tables 1−3. On the basis of similarities in the NMR spectra the molecule is structurally akin to **6a**. In the ^{31}P{^{1}H} NMR spectrum of **6b** there are two resonances: a singlet at δ 40.0 due to the Ru(PPh_3) group and a pair of doublets at δ 13.8 assignable to the Ag-(PPh_3) group on the basis of the ^{107}Ag− and ^{109}Ag−^{31}P couplings (Table 3).[13]

In further confirmation a unit cell measurement of a single crystal of **6b** revealed the presence of a solvent molecule, as with **6a**, and the three comparable axial lengths and interaxial angles. Since the unit cells of **6a** and **6b** are equivalent in both size and shape, and have similar volumes, the two species can be assumed to be isostructural.

Treatment of **4b** with [AuCl(PPh_3)] in thf in a 1:1 mole ratio in the presence of $TlPF_6$ afforded the compound $[Ru_3(\mu\text{-H})(CO)_8\{\eta^5\text{-10-Au}(PPh_3)\text{-7-}CB_{10}H_{10}\}]$ (**6c**), data for which are summarized in Tables 1−3. A single-crystal X-ray diffraction study gave the structural parameters listed in Table 6 , and the molecule is shown in Figure 3. This study confirmed the presence of the Au(PPh_3) substituent attached to the cage at B(3) and, importantly, the absence of any B−H⇀Au interaction similar to that involving B(8) and the copper atom in **6a** (Figure 2). The ^{13}C{^{1}H} NMR spectrum of this asymmetric molecule displayed eight CO signals, as expected (Table 2). One resonance at δ 196.3 was very broad and is tentatively assigned to C(23)O(23) transoid to B(3) (Figure 3), the broadness of the signal being ascribed to ^{11}B coupling. Another resonance at δ 192.4 was a doublet (J(PC) = 9 Hz) and is assigned to C(33)O-(33) transoid to the Au(PPh_3) group.

Thus, in **6c** both the Ru(2) and the Ru(3) atoms carry three terminal CO groups. The Ru(PPh_3) groups present in **6a** and **6b** must be attributed to the presence of free PPh_3 during the synthesis of these molecules. For **6a** an excess of [$CuCl(PPh_3)_3$] was used, a reagent from which PPh_3 dissociates. In the preparation of **6b** free PPh_3 was added as a reagent and would thus be present in the mixtures. Interestingly, treatment of a sample of **6c** with PPh_3 unexpectedly afforded a salt rather than a neutral species $[Ru_3(\mu\text{-H})(CO)_7(PPh_3)\{\eta^5\text{-10-Au}(PPh_3)\text{-7-}CB_{10}H_{10}\}]$ akin to **6a**,**b**. We formulate the salt as $[Au(PPh_3)_3][Ru_3(CO)_8(\eta^5\text{-7-}CB_{10}H_{11})]$ (**4c**). The ^{11}B{^{1}H} NMR spectrum was identical with that of **4a**. The ^{31}P{^{1}H} NMR spectrum showed a singlet at δ 31.1, which we ascribe to the tricoordinate gold cation $[Au(PPh_3)_3]^+$. Although this cation has been characterized by X-ray crystallography,[14] its ^{31}P{^{1}H} NMR spectrum does not seem to have been previously reported. However, the value δ 31.1 is to higher field than that for $[Au(PPh_3)_2]^+$ (δ 45.2),[15] in accord with the gold center being bound to three rather than four phosphorus atoms. Formation of

(13) Muetterties, E. L.; Alegranti, C. W. *J. Am. Chem. Soc.* **1972**, *94*, 6386.

(14) Guggenberger, L. J. *J. Organomet. Chem.* **1974**, *81*, 271.

(15) Carriedo, G. A.; Howard, J. A. K.; Stone, F. G. A.; Went, M. J. *J. Chem. Soc., Dalton Trans.* **1984**, 2545.

Table 6. Selected Internuclear Distances (Å) and Angles (deg) for $[Ru_3(\mu\text{-H})(CO)_8\{\eta^5\text{-10-Au}(PPh_3)\text{-7-}CB_{10}H_{10}\}]$ (6c)

Ru(1)−C(12)	1.905(13)	Ru(1)−C(11)	1.913(13)	Ru(1)−B(4)	2.229(12)	Ru(1)−B(3)	2.234(13)
Ru(1)−B(5)	2.239(13)	Ru(1)−B(2)	2.273(13)	Ru(1)−C(1)	2.255(11)	Ru(1)−Ru(2)	2.7607(14)
Ru(1)−Ru(3)	2.774(2)	Ru(2)−H(3)	1.78(5)	Ru(2)−H(23)	1.61(4)	Ru(2)−C(21)	1.92(2)
Ru(2)−C(23)	1.930(13)	Ru(2)−C(22)	1.938(14)	Ru(2)−B(3)	2.387(13)	Ru(2)−Ru(3)	3.004(2)
Ru(3)−C(31)	1.904(14)	Ru(3)−C(33)	1.931(14)	Ru(3)−C(32)	1.919(14)	Ru(3)−B(4)	2.336(12)
Ru(3)−H(23)	1.63(5)	Ru(3)−Au	2.7186(13)	B(4)−Au	2.293(12)	Au−P	2.295(3)
C(11)−O(11)	1.152(14)	C(12)−O(12)	1.155(13)	C(23)−O(23)	1.131(14)	C(22)−O(22)	1.105(14)
C(21)−O(21)	1.138(14)	C(31)−O(31)	1.147(14)	C(32)−O(32)	1.124(14)	C(33)−O(33)	1.139(14)

C(12)−Ru(1)−C(11)	88.4(5)	C(12)−Ru(1)−Ru(2)	81.6(3)	C(11)−Ru(1)−Ru(3)	81.4(4)
C(11)−Ru(1)−Ru(2)	127.7(4)	C(12)−Ru(1)−Ru(3)	127.4(4)	Ru(2)−Ru(1)−Ru(3)	65.74(4)
C(21)−Ru(2)−C(22)	93.6(5)	C(21)−Ru(2)−C(23)	90.5(5)	C(23)−Ru(2)−C(22)	95.9(5)
C(23)−Ru(2)−Ru(1)	95.5(4)	C(21)−Ru(2)−Ru(1)	98.2(4)	C(22)−Ru(2)−Ru(1)	163.6(4)
C(23)−Ru(2)−Ru(3)	89.0(4)	C(21)−Ru(2)−Ru(3)	155.4(4)	C(22)−Ru(2)−Ru(3)	111.0(4)
C(31)−Ru(3)−C(33)	94.9(5)	C(31)−Ru(3)−C(32)	91.6(5)	Ru(1)−Ru(2)−Ru(3)	57.34(3)
C(32)−Ru(3)−Au	70.0(4)	C(31)−Ru(3)−Au	80.2(3)	C(32)−Ru(3)−C(33)	94.3(5)
C(31)−Ru(3)−Ru(1)	98.5(4)	B(4)−Ru(3)−Au	53.3(3)	C(33)−Ru(3)−Au	163.2(4)
C(33)−Ru(3)−Ru(1)	92.4(4)	Au−Ru(3)−Ru(1)	104.10(4)	C(32)−Ru(3)−Ru(1)	167.3(4)
C(31)−Ru(3)−Ru(2)	155.3(4)	C(33)−Ru(3)−Ru(2)	89.2(4)	C(32)−Ru(3)−Ru(2)	112.4(4)
O(11)−C(11)−Ru(1)	176.1(11)	Au−Ru(3)−Ru(2)	101.97(4)	Ru(1)−Ru(3)−Ru(2)	56.92(4)
O(21)−C(21)−Ru(2)	177.6(12)	O(12)−C(12)−Ru(1)	176.7(11)	O(22)−C(22)−Ru(2)	179.1(12)
O(33)−C(33)−Ru(3)	175.7(11)	O(23)−C(23)−Ru(2)	178.9(12)	O(31)−C(31)−Ru(3)	177.5(10)
B(4)−Au−P	149.0(3)	O(32)−C(32)−Ru(3)	173.9(12)	Ru(1)−B(4)−Au	146.6(6)
P−Au−Ru(3)	156.12(8)	Au−B(4)−Ru(3)	71.9(4)	B(4)−Au−Ru(3)	54.8(3)

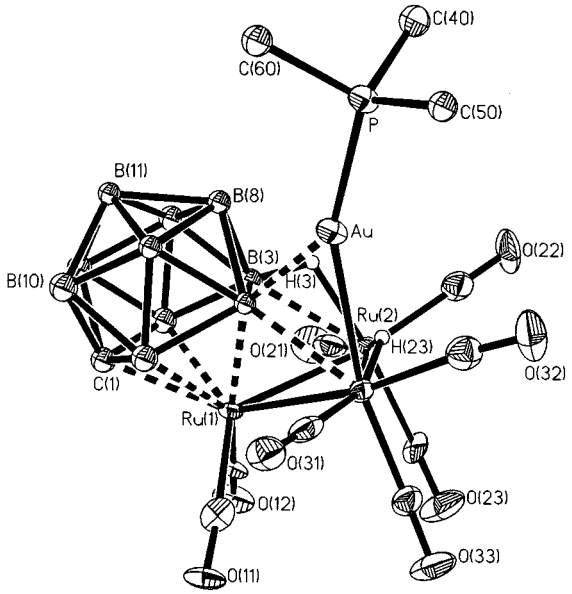

Figure 3. Structure of $[Ru_3(\mu\text{-H})(CO)_8\{\eta^5\text{-10-Au}(PPh_3)\text{-7-}CB_{10}H_{10}\}]$ (**6c**), showing the crystallographic labeling scheme. Thermal ellipsoids are shown at the 40% probability level. Only the agostic hydrogen atom H(3), H(23) bridging the Ru(2)−Ru(3) bond, and the C^1 atoms of the phenyl rings are shown are shown for clarity.

4c from **6c** and PPh_3 perhaps reflects the thermodynamic stability of $[Au(PPh_3)_n]^+$ cations.[16]

Conclusions

In the salts **4** and in the hydrido complex **5** the carborane cage framework formally contributes 7 valence electrons to the clusters, and these together with 16 electrons from the CO ligands and 24 from the metal atoms provide 47 of the 48 valence electrons necessary for a closed-shell configuration. For **4** and **5** the additional electron required is derived from the anionic charge in the former and the hydrido ligand in the latter. The relationship between **5** and **2**, and between **5** and **3a**, follows naturally from the *nido*-7-$CB_{10}H_{11}$ ligand in **5** functioning as a 7-electron donor to the metal triangle, whereas the cage frameworks *nido*-7,8-$Me_2C_2B_9H_9$ in **2** and *nido*-7-NMe_3-7-$CB_{10}H_{10}$ in **3a**, respectively, donate 8 electrons toward the overall electron count in these clusters.

To our knowledge, the molecular structures of the three cluster complexes **6** have no precedent at the present time. The structural relationship between **5** and **6c** is of particular interest. The replacement of a μ-H group in a M(μ-H)M system by the isolobal μ-Au(PPh_3) group was first recognized 20 years ago,[17] and the methodology was subsequently developed to prepare many heteronuclear metal clusters with μ-Au(PR_3) groups.[18] Hence, treatment of **4b** with $[Au(PPh_3)]^+$ might have been anticipated to yield a molecule wherein the gold fragment bridges a Ru−Ru bond as does the bridging hydrido ligand H(23) of **5** (Figure 1). However, **6c** has a structure in which one of the B−H⇀Ru agostic bonds of **4b** is replaced by a B−Au(PPh_3)⇀Ru bridge with generation of a Ru(μ-H)Ru unit as in **5**. It is noteworthy that three-center bridge bonding by a Au(PPh_3) fragment has precedent in other structures.[15,19]

Although in most respects the structures of the molecules **6a**−**c** are similar, **6a** and **6b** have the additional feature of a B−H⇀M (M = Cu or Ag) exopolyhedral bridge. The existence of this agostic bond contributes a further two electrons to the Cu and Ag centers. The absence of such a bond in the gold complex may be traced to the relative differences in the energies of the three unoccupied frontier molecular orbitals in the fragments M(PPh_3) (M = Cu, Ag, Au). As discussed elsewhere,[20,21] for gold only one such orbital is energetically suitable for bonding, whereas for copper, and

(16) Gimeno, M. C.; Laguna, A. *Chem. Rev.* **1997**, *97*, 511.

(17) Farrugia, L. J.; Howard, J. A. K.; Mitrprachachon, P.; Spencer, J. L.; Stone, F. G. A.; Woodward, P. *J. Chem. Soc., Chem. Commun.* **1978**, 260. Howard, J. A. K., Salter, I, D., Stone, F. G. A. *Polyhedron* **1984**, *3*, 567.

(18) Salter, I. D. *Adv. Organomet. Chem.* **1989**, *29*, 249.

(19) Jeffery, J. C.; Jelliss, P. A.: Stone, F. G. A. *J. Chem. Soc., Dalton Trans.* **1993**, 1083.

(20) Evans, D. G.; Mingos, D. M. P. *J. Organomet. Chem.* **1982**, *232*, 171.

(21) Hamilton, E. J. M.; Welch, A. J. *Polyhedron* **1990**, *9*, 2407.

evidently for silver also, all three are accessible for bond formation. This property is well-illustrated by the two molecules $[PtM(PEt_3)_2(PPh_3)(\eta^5\text{-}7\text{-}CB_{10}H_{11})]$ (M = Cu, Au); in the copper species the Pt−Cu bond is supported by two exopolyhedral B−H⇀Cu linkages, whereas in the gold complex **6c** the Pt−Au bond stands alone.[10b]

Experimental Section

General Considerations. Solvents were distilled from appropriate drying agents under nitrogen prior to use. Petroleum ether refers to that fraction of boiling point 40−60 °C. All reactions were carried out under an atmosphere of dry nitrogen using Schlenk line techniques. Chromatography columns (ca. 15 cm in length and ca. 2 cm in diameter) were packed with silica gel (Aldrich, 70−230 mesh). TLC was performed on preparative UNIPLATES (silica gel G, Analtech). NMR spectra were recorded at the following frequencies: ^{1}H, 360.1 MHz; ^{13}C, 90.6 MHz; ^{31}P, 145.7 MHz; ^{11}B, 115.5 MHz. The salt $[NHMe_3][nido\text{-}7\text{-}CB_{10}H_{13}]$ was synthesized from *nido*-7-Me_3N-7-$CB_{10}H_{12}$ according to the method of Knoth et al.[22] The complexes $[AuCl(PPh_3)]$[23] and $[CuCl(PPh_3)_3]$[24] were prepared according to the literature methods.

Synthesis of $[PPh_4][Ru_3(CO)_8(\eta^5\text{-}7\text{-}CB_{10}H_{11})]$. The compounds $[Ru_3(CO)_{12}]$ (0.32 g, 0.50 mmol) and $[NHMe_3][nido\text{-}7\text{-}CB_{10}H_{13}]$ (0.10 g, 0.50 mmol) were heated at reflux in thf (10 mL) for 24 h to generate the salt **4b** in situ. The mixture was then cooled to room temperature, and $[PPh_4]Br$ (0.42 g, 1 mmol) was added. Solvent was removed in vacuo, and the residue was treated with CH_2Cl_2 (15 mL). After filtration through a Celite plug ca. 2 g of silica gel was added to the filtrate. Solvent was removed in vacuo, affording an orange powder which was transferred to the top of a chromatography column. Elution with CH_2Cl_2 removed an orange fraction. Removal of solvent in vacuo yielded orange microcrystals of $[PPh_4][Ru_3(CO)_8(\eta^5\text{-}7\text{-}CB_{10}H_{11})]$ (**4a**; 0.43 g).

Protonation of $[NHMe_3][Ru_3(CO)_8(\eta^5\text{-}7\text{-}CB_{10}H_{11})]$. The compounds $[Ru_3(CO)_{12}]$ (0.32 g, 0.50 mmol) and $[NHMe_3][nido\text{-}7\text{-}CB_{10}H_{13}]$ (0.10 g, 0.50 mmol) were heated at reflux in thf (10 mL) for 24 h to generate the salt **4b**. The mixture was then cooled to room temperature, and $HBF_4{\cdot}OEt_2$ (0.10 mL) was added. Solvent was removed in vacuo, and the residue was treated with CH_2Cl_2 (15 mL). After filtration through a Celite plug ca. 2 g of silica gel was added. Solvent was removed in vacuo, affording a reddish powder which was transferred to the top of a chromatography column. Elution with CH_2Cl_2−petroleum ether (1:1) gave an orange fraction. Removal of solvent in vacuo followed by crystallization from CH_2Cl_2−petroleum ether yielded orange microcrystals of $[Ru_3(\mu\text{-}H)(CO)_8(\eta^5\text{-}7\text{-}CB_{10}H_{11})]{\cdot}CH_2Cl_2$ (**5**; 0.30 g).

Synthesis of the Triruthenium−Copper, −Silver, and −Gold Complexes. (i) The compounds $[Ru_3(CO)_{12}]$ (0.32 g, 0.50 mmol) and $[NHMe_3][nido\text{-}7\text{-}CB_{10}H_{13}]$ (0.10 g, 0.50 mmol) were heated at reflux in thf (10 mL) for 24 h to generate **4b** in situ. The mixture was then cooled to 0 °C, and $[CuCl(PPh_3)_3]$ (0.86 g, 1.00 mmol) and $TlPF_6$ (0.35 g, 1.0 mmol) were added. After the mixture was stirred at room temperature for ca. 12 h, solvent was removed in vacuo and the dark red residue was taken up in CH_2Cl_2 (15 mL). After filtration through Celite ca. 2 g of silica gel was added to the filtrate, solvent was removed in vacuo, and the reddish powder obtained was transferred to the top of a chromatography column. Elution with CH_2Cl_2−petroleum ether (1:1) gave an orange fraction. Removal of solvent in vacuo followed by crystallization from CH_2Cl_2−petroleum ether yielded orange microcrystals of $[Ru_3(\mu\text{-}H)(CO)_7(PPh_3)\{\eta^5\text{-}10\text{-}Cu(PPh_3)\text{-}7\text{-}CB_{10}H_{10}\}]$ (**6a**; 0.27 g).

(ii) The compounds $[Ru_3(CO)_{12}]$ (0.32 g, 0.50 mmol) and $[NHMe_3][nido\text{-}7\text{-}CB_{10}H_{13}]$ (0.10 g, 0.50 mmol) were heated at reflux in thf (10 mL) for 24 h. The mixture was then cooled to −78 °C, and PPh_3 (0.26 g, 1.0 mmol) and $Ag[BF_4]$ (0.19 g, 1.0 mmol) were added. The reactants were stirred at room temperature for ca. 12 h, after which solvent was removed in vacuo and the dark red residue was treated with CH_2Cl_2 (15 mL). After filtration silica gel (ca. 2 g) was added to the filtrate. Solvent was removed in vacuo, affording a reddish powder which was transferred to the top of a chromatography column. Elution with CH_2Cl_2−petroleum ether (1:1) gave an orange fraction. Removal of solvent in vacuo followed by crystallization from CH_2Cl_2−petroleum ether yielded orange microcrystals of $[Ru_3(\mu\text{-}H)(CO)_7(PPh_3)\{\eta^5\text{-}10\text{-}Ag(PPh_3)\text{-}7\text{-}CB_{10}H_{10}\}]$ (**6b**; 0.24 g).

(iii) The compounds $[Ru_3(CO)_{12}]$ (0.32 g, 0.50 mmol) and $[NHMe_3][nido\text{-}7\text{-}CB_{10}H_{13}]$ (0.10 g, 0.50 mmol) were heated at reflux in thf (10 mL) for 24 h. The mixture was then cooled to 0 °C, and $[AuCl(PPh_3)]$ (0.25 g, 0.5 mmol) and $TlPF_6$ (0.17 g, 0.5 mmol) were added. After the mixture was stirred at room temperature for ca. 12 h, solvent was removed in vacuo and the dark red residue was taken up in CH_2Cl_2 (15 mL). After filtration through a Celite plug, silica gel (ca. 2 g) was added, solvent was removed in vacuo, and the reddish powder obtained was transferred to the top of a chromatography column. Elution with CH_2Cl_2−petroleum ether (1:1) gave an orange fraction. Removal of solvent in vacuo followed by crystallization from CH_2Cl_2−petroleum ether yielded orange microcrystals of $[Ru_3(\mu\text{-}H)(CO)_8\{\eta^5\text{-}10\text{-}Au(PPh_3)\text{-}7\text{-}CB_{10}H_{10}\}]$ (**6c**; 0.35 g).

Crystal Structure Determinations and Refinements. Suitable crystals of **5**, **6a**, and **6c** were grown by diffusion of CH_2Cl_2 solutions into petroleum ether. Experimental data are summarized in Table 7. Data sets were collected at low temperature (−100 °C) for **5** and **6c** and at room temperature for **6a**. For **5** and **6a** diffracted intensities were recorded on an Enraf-Nonius CAD-4 instrument operating in $\omega-(2/3)\theta$ (**5**) and $\omega-\theta$ (**6a**) scan modes, using graphite-monochromated Mo Kα X-radiation ($\bar{\lambda}$ = 0.710 73 Å). The final unit cell dimensions were determined from the setting angle values of 25 accurately centered reflections. The stability of the crystal during the period of the data collection was monitored by measuring the intensities of three standard reflections every 2 h. Data were collected at a constant scan speed of 5.17° min^{-1} in ω, with a scan range of 1.15° + 0.35 tan θ. The data were corrected for Lorentz, polarization, and X-ray absorption effects, the last by a semiempirical method based on azimuthal scans of ψ data.

A single crystal of **6c** was mounted on a glass fiber, and data were collected on a Siemens SMART CCD area-detector three-circle diffractometer using Mo Kα X-radiation, $\bar{\lambda}$ = 0.710 73 Å. For three settings of ϕ, narrow data "frames" were collected for 0.3° increments in ω. In this case a total of 2082 frames of data were collected, affording approximately a sphere of data. It was confirmed that crystal decay had not taken place during the course of the data collections. The substantial redundancy in data allows empirical absorption corrections (SADABS)[25] to be applied using multiple measurements of equivalent reflections. The data frames were integrated using the SAINT[25] program.

All structures were solved by direct methods, and successive Fourier difference syntheses were used to locate all non-hydrogen atoms, using SHELXTL-PC version 4.1 or SHELXTL version 5.03.[25] All non-hydrogen atoms, except for those described below, were assigned anisotropic thermal parameters and refined without geometric constraints. Complexes **5** and **6a** contained a disordered molecule of dichloromethane in the asymmetric unit. In each case the carbon atom was constrained to have the same positional and thermal parameters, while the chlorine atoms occupied two sites with occupancies of 0.54(4), 0.46(4) in **5** and 0.73(2), 0.27(2) in **6a**.

(22) Knoth, W. H.; Little, J. L.; Lawrence, J. R.; Scholer, F. R.; Todd, L. J. *Inorg. Synth.* **1968**, *11*, 33.
(23) Usón, R.; Laguna, A. *Organomet. Synth.* ***1986***, *3*, 324.
(24) Stephens, R. D. *Inorg. Synth.* **1979**, *19*, 87.
(25) Bruker AXS Inc., Madison, WI, 1995.

Table 7. Data for X-ray Crystal Structure Analyses

	5·CH_2Cl_2	**6a**·CH_2Cl_2	**6c**
cryst dimens (mm)	0.20 × 0.10 × 0.10	0.10 × 0.10 × 0.08	0.10 × 0.08 × 0.08
formula	$C_{10}H_{14}B_{10}Cl_2O_8Ru_3$	$C_{45}H_{43}B_{10}Cl_2CuO_7P_2Ru_3$	$C_{27}H_{26}AuB_{10}O_8PRu_3$
M_r	744.42	1303.48	1117.72
cryst color, shape	orange blocks	orange-red prisms	dark red plates
cryst system	monoclinic	triclinic	triclinic
space group	$P2_1/n$	$P\bar{1}$	$P\bar{1}$
a (Å)	10.7007(27)	12.9133(25)	12.222(4)
b (Å)	18.2950(36)	14.3357(26)	13.027(3)
c (Å)	12.9736(30)	15.8791(27)	13.317(3)
α (deg)		102.307(12)	80.48(2)
β (deg)	102.619(21)	106.774(17)	82.25(2)
γ (deg)		100.541(18)	62.98(2)
V (Å$^{3)}$	2478.5(10)	2654.3(8)	1858.7(8)
Z	4	2	2
d_{calcd} (g cm^{-3})	1.995	1.631	1.997
μ(Mo Kα) (cm^{-1})	20.54	14.40	52.17
F(000) (e)	1416	1288	1056
T (K)	173	293	173
2θ range (deg)	4.5−50.0	3.0−48.0	3.5−48.0
no. of rflns coll (excld stds)	4573	8737	14 620
no. of unique rflns	4332	8314	5802
no. of obsvd rflns	3770	5483	3975
reflection limits: h, k, l	0−12; 0−21; −15 to +14	−15 to 0; −16 to +17; −18 to +18	−15 to 15; −16 to +16; −17 to +17
no. of params refined	330	652	314
final residuals wR2 (R1), all data	0.0758 (0.0385)[a]	0.0996 (0.0983)[a]	0.1193 (0.0863)[a]
weighting factors[a]	a = 0.0289, b = 6.3354	a = 0.0317, b = 0.000	a = 0.0540, b = 0.000
goodness of fit on F^2	1.107	1.016	0.989
max, min final electron density diff features (e Å^{-3})	0.514, −0.441	0.492, −0.523	2.182, −2.264

[a] Refinement was block full-matrix least squares on all F^2 data: wR2 = $[\sum\{w(F_o^2 - F_c^2)^2\}/\sum w(F_o^2)^2]^{1/2}$, where $w^{-1} = [\sigma^2(F_o^2) + (aP)^2 + bP]$ and $P = [\max(F_o^2,0) + 2F_c^2]/3$. The value in parentheses is given for comparison with refinements based on F_o with a typical threshold of $F_o > 4\sigma(F_o)$ and R1 = $\sum||F_o^2| - |F_c||/\sum|F_o|$ and $w^{-1} = [\sigma^2(F_o) + g(F_o^2)]$.

In **6a**, the disordered chlorine atoms were refined with isotropic thermal parameters. The crystal quality of **6c** was less than ideal, and data were relatively weak, precluding full anisotropic refinement of all the non-hydrogen atoms; hence, only the metal atoms, carbonyl groups, and phosphorus atoms were assigned anisotropic thermal parameters. The remaining atoms were refined with isotropic thermal parameters.

With the exception of the bridging Ru(μ-H)Ru and agostic B−H⇀Ru protons, all hydrogen atoms were included in calculated positions and allowed to ride on the parent boron or carbon atoms with isotropic thermal parameters (U_{iso} = 1.2 times the U_{iso} value of the parent atom, except for methyl protons, where U_{iso} = 1.5U_{iso}). The agostic B−H⇀Ru hydrogen atoms and bridging Ru(μ-H)Ru hydrogen atoms in **5** and **6a** were located in difference Fourier syntheses, and their positions and isotropic thermal parameters were refined. Due to the crystal quality in **6c** both agostic and bridging hydrogen atoms were located using the energy minimization program XHYDEX[26] and refined with geometric positional restraints. Refinements were made by full-matrix least-squares on F^2 data, and atomic scattering factors were taken from ref 27. The final electron-density difference syntheses for **6c** showed significant residual peaks in the vicinity of the transition-metal atoms and reflect the comparatively poor quality of crystals available for data collection and an inability to correct completely for absorption effects. All calculations were carried out on Silicon Graphics Indy or Dell PC computers.

An analysis of a single crystal of **6b** revealed the presence of a CH_2Cl_2 molecule and a unit cell with three axial lengths and three inter axial angles (crystal data: triclinic, a = 12.974(26) Å, b = 14.218(9) Å, c = 16.256(24) Å, α = 101.66(8)°, β = 108.60(16)°, γ = 101.22(11)°, V = 2672.3(28) Å^3) comparable with those of **6a** (Table 7). Furthermore, when considering the atomic radii of Cu and Ag, it should be expected that there will be some differences in the experimental lattice constants determined, but these values are consistent within experimental error.

Acknowledgment. We thank the Robert A. Welch foundation for support (Grant AA-1201) and Dr. Paul Jelliss for helpful advice.

Supporting Information Available: Tables of atomic coordinates and U values, bond lengths and angles, and anisotropic thermal parameters for **5**, **6a**, and **6c** in CIF format. This material is available free of charge via the Internet at http://pubs.acs.org.

OM990133X

(26) Orpen, A. G. *J. Chem. Soc., Dalton Trans.* **1980**, 2509.
(27) *International Tables for X-ray Crystallography*; Kynoch Press: Birmingham, U.K., 1974; Vol. 4.